ACS Medicinal Chemistry Letters

pubs.acs.org/acsmedchemlett Letter

A Set of Highly Sensitive Sirtuin Fluorescence Probes for Screening Small-Molecular Sirtuin Defatty-Acylase Inhibitors

Yuya Nakajima, Mitsuyasu Kawaguchi,* Naoya Ieda, and Hidehiko Nakagawa*

Cite This: *ACS Med. Chem. Lett.* 2021, 12, 617−624 Read Online

ACCESS | Metrics & More | Article Recommendations | Supporting Information

ABSTRACT: Human sirtuins (SIRT1−7) regulate not only deacetylation but also deacylation of fatty acid-derived acyl moieties (defatty-acylation) at the ε-amino group of lysine residues. SIRT-subtype-specific defatty-acylase activity modulators are needed for detailed investigation of the biological roles of these enzymes, and to find suitable small molecules, we require appropriate screening systems. Here, we designed and synthesized a set of SIRT defatty-acylase activity probes with various quencher moieties and peptide sequences based on our previously developed one-step FRET-based SIRT probe SFP3, using improved methodology. Scanning of this set of probes with SIRT isozymes revealed that certain probe/isozyme combinations showed especially high responses. To illustrate the utility of the combinations thus identified, we applied compound **18**/SIRT2 for inhibitor screening of a large chemical library. This enabled us to discover a new small molecule SIRT2-specific defatty-acylase inhibitor.

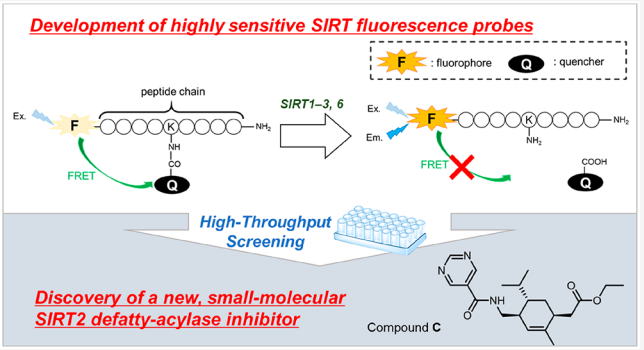

KEYWORDS: *sirtuin, fluorescence probes, defatty-acylase activity, screening, inhibitors*

Human sirtuins (SIRT1−7) are a family of NAD^+-dependent histone deacetylases.[1] SIRTs are involved in metabolic regulation, stabilization of genomic DNA, stress responses, and even aging,[2−6] and SIRT modulators are considered to have potential therapeutic value.[7−10] For a long time, it was thought that SIRTs only catalyze deacetylation reactions of histones and the adenine diphosphate (ADP)-ribosylation reaction. However, more recently, it was found that SIRTs can remove various acyl groups, including propionyl, butyryl, crotonyl, succinyl, hexanoyl, octanoyl, decanoyl, dodecanoyl, myristoyl, palmitoyl, lipoyl, and benzoyl groups,[11,12] from histones and many other protein substrates.[13,14] SIRT1−3, which have relatively potent deacetylase activity, can also remove long-chain fatty acyl groups at the ε-amino group of lysine residues *in vitro*.[11,12]

Protein fatty-acylation is crucial for anchoring proteins to the cell membrane and plays important roles in cell signaling and protein−protein interactions. Early studies of protein fatty acylation were focused on *N*-terminal glycine myristoylation and cysteine palmitoylation.[15,16] Among human SIRTs, SIRT6 is a prominent defatty-acylase, which regulates secretion of tumor necrosis factor α (TNF-α) and exosomes.[17−19] Recent work suggests that the defatty-acylase activity of SIRT2 toward the ε-amino group of lysine residues regulates the localization of K-Ras4a oncoprotein[20] and promotes cellular transformation via interaction with A-Raf.[20] In addition to K-Ras4a, the defatty-acylase activity of SIRT2 regulates the activity of RalB and cell migration.[21] Therefore, SIRT2 defatty-acylase activity plays an important role in cancer proliferation. However, so far, there has been no report on the physiological roles of the defatty-acylase activities of SIRT1 and SIRT3. Therefore, SIRT-subtype-specific modulators are required both as tools for basic research to understand the physiological functions of SIRTs and as candidate therapeutic agents.

So far, SIRT fluorescent probes employing various detection methods have been developed. Generally, they involve trypsin digestion of a *C*-terminal lysine residue after the SIRT enzymatic reaction.[22,23] However, this requirement is problematic for screening purposes because trypsin inhibitors generate false-positive signals. Therefore, a one-step procedure for detection of SIRT activity would be preferable. Some one-step probes employing an intramolecular reaction mechanism, which affords a fluorescence increase after deacylation of a lysine residue, have been reported,[24−26] but unfortunately, the background fluorescence signal gradually increases even in the absence of enzymes. Dai and coworkers[27] developed a Förster resonance energy transfer (FRET)-based fluorescence probe containing a 2-aminobenzoylamide group at the acyl side chain

Received: January 8, 2021
Accepted: March 9, 2021
Published: March 11, 2021

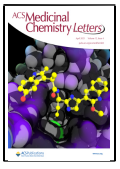

https://dx.doi.org/10.1021/acsmedchemlett.1c00010
ACS Med. Chem. Lett. 2021, 12, 617−624

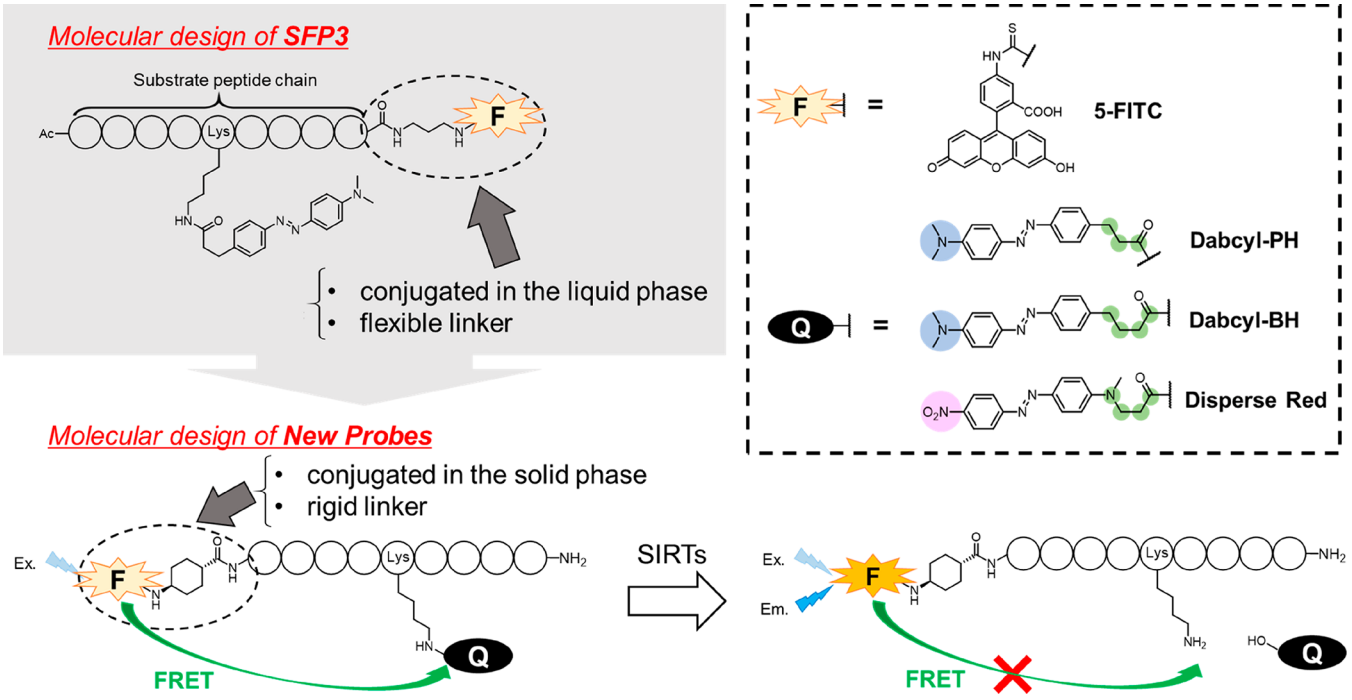

Figure 1. Molecular design strategy and function of newly designed one-step SIRT activity probes employing the FRET mechanism.

as a fluorophore. Its fluorescence is activated by SIRT-mediated hydrolytic release of the fluorophore moiety, but the absorption and fluorescence wavelengths of the fluorophore, 2-aminobenzoylamide, are quite short and may overlap with those of chemical compounds to be screened. Therefore, there is still a need for a stable, one-step fluorescence probe with a longer fluorescence wavelength for chemical screening purposes.

We have already reported a one-step chemical probe for SIRT activity, SFP3, which can evaluate the defatty-acylase activity of SIRT1−3 and SIRT6 (Figure S1).[28] SFP3 is a FRET-based fluorescence probe containing a 4-(4-dimethylaminophenylazo)benzoyl (Dabcyl) group as a quencher, and its fluorescence is activated by SIRT-mediated hydrolytic release of the Dabcyl moiety, as shown in Figure 1. The long structure of the Dabcyl group appears to mimic a long-chain fatty acyl group because the K_m values of the Dabcyl quencher and the myristoyl group are similar.[28,29] However, for purposes such as high-throughput chemical screening and subtype-specific imaging of cellular SIRT, it would be useful to have a set of probes with different characteristics. Therefore, in this work, we set out to build a set of probes incorporating various peptide sequences and quenchers using improved synthetic methodology (Figure 1). We evaluated the kinetic parameters of the obtained probes toward SIRT1−7 and compared them with the corresponding parameters of SFP3. We found that certain combinations of probes and isozymes showed especially high responses, supporting the value of our approach for developing SIRT-subtype-specific probes. We confirmed its practical utility by applying one of the new probes, **18**, which showed especially high sensitivity to SIRT2, for SIRT2 inhibitor screening. This enabled us to discover a new small molecule SIRT2 defatty-acylase inhibitor.

RESULTS AND DISCUSSION

Molecular Design Strategy for New SIRT Activity Probes. For the development of the new fluorescence probes, we modified the original design and synthetic scheme used for our previously reported probe, SFP3,[28,29] as shown in Figure 1. In SFP3, the linker and fluorophore were conjugated at the *C*-terminus of the H3K9 peptide, which was obtained by solid-phase synthesis (SPS). However, the linker and fluorophore moieties were subsequently conjugated in the liquid phase, which requires an increased number of synthetic steps, resulting in a low yield and many byproducts. In our new design, the linker and fluorophore are conjugated at the *N*-terminus of the peptide chain, and the scheme was modified to allow all the components to be incorporated by means of SPS. In addition, SFP3 showed unwanted interactions (e.g., intramolecular stacking interactions) between the fluorophore and the quencher group due to its highly flexible propyl linker. In our new design, the linker structure was changed to a more rigid cyclohexane ring with the aim of preventing such stacking interactions and increasing the reactivity with SIRTs.

According to the above strategy, we designed **13** with a 9-residue H4K16 peptide as a substrate peptide and Dabcyl-PH as a quencher, followed by **14** and **15**, which have a 7- and an 11-residue H4K16 peptide, respectively. We next designed **16** and **17**, which contain the "RIKRY" sequence of peptide-type SIRT2-selective inhibitors (S2iL8, S2iD7),[30] anticipating that these sequences would increase the binding affinity to SIRT2. Our previous findings indicated that a longer linker structure of the Dabcyl group increases the reactivity with SIRT.[28] Thus, we next designed **18** with Dabcyl-BH as a quencher, which is longer by one carbon atom than Dabcyl-PH. We then considered the influence of the electron density of the quencher group. All the above probes have Dabcyl-type quenchers with an electron-donating dimethylamino group at the end of the structure. We thus designed **19**, which contains an H4K16 peptide and a Disperse Red quencher moiety

https://dx.doi.org/10.1021/acsmedchemlett.1c00010
ACS Med. Chem. Lett. 2021, 12, 617−624

bearing an electron-withdrawing nitro group at the end of the structure. We also designed **20**–**23** containing peptide sequences RIKRY, RalB, H2BK12, and H3K9 with a Disperse Red quencher. The characteristics of these probes are summarized in Table 1.

Table 1. Structures of Quenchers and Peptides Used in the New Probes

	quencher	peptide sequence	length
SFP3	Dabcyl-PH	H3K9 (QTARKSTGG)	9 residues
13	Dabcyl-PH	H4K16 (KGGAKRHRK)	9 residues
14	Dabcyl-PH	H4K16 (GGAKRHR)	7 residues
15	Dabcyl-PH	H4K16 (GKGGAKRHRKV)	11 residues
16	Dabcyl-PH	S2iL8 (NFRIKRYSN)	9 residues
17	Dabcyl-PH	S2iD7 (DYRIKRYHT)	9 residues
18	Dabcyl-BH	H4K16 (KGGAKRHRK)	9 residues
19	Disperse Red	H4K16 (KGGAKRHRK)	9 residues
20	Disperse Red	S2iD7 (DYRIKRYHT)	9 residues
21	Disperse Red	RalB (KKSFKERSS)	9 residues
22	Disperse Red	H2BK12 (APAPKKGSK)	9 residues
23	Disperse Red	H3K9 (QTARKSTGG)	9 residues

Synthesis of FRET-Based SIRT Activity Probes 13–23. **13**–**23** were synthesized as shown in Scheme S1. Dabcyl-PH (**3**), Dabcyl-BH (**6**), and Disperse Red (**10**) were synthesized and conjugated with Fmoc-Lys-OH in 4, 3, and 4 steps, respectively. Finally, each probe was obtained by Fmoc solid-phase synthesis on Sieber amide resin, cleaved, and purified by preparative reversed-phase HPLC (purity: >95%). The structures were confirmed by HRMS.

Photochemical Properties of 13–23. We measured the absorption and fluorescence spectra and calculated the fluorescence quantum yields of all the synthesized probes (Figure 2, Table 2). The absorption spectrum of each probe showed overlapping absorbance of FITC and the quencher dye, and the fluorescence spectra indicated that the fluorescence of each probe was sufficiently quenched by the FRET mechanism compared to the reference, 5-FITC (Figure 2B).

Reactivity of 13–23 with SIRT1–7. Next, we examined the reactivity of each probe with SIRT1–7 by means of enzymatic assay in 96-well half area plates at 37 °C for 1 h. The values of fluorescence enhancement (fold change) after 1 h are shown in Table 3 and Figure S2.

Most of the probes reacted with SIRT1, SIRT2, and SIRT3, and some showed a large fluorescence enhancement (>10-fold) after 1 h enzymatic reaction. In contrast, none of the probes reacted significantly with SIRT4, 5, or 7, suggesting that our quencher-hydrolyzing strategy might not be suitable for detection of their activities. In the case of SIRT6, several probes, including **22** and **23**, showed moderate to high reactivity compared to SFP3. This result suggests that the peptide sequence, especially H3K9, may be critical for improving the binding affinity with SIRT6, and the Disperse Red quencher may be more suitable than the Dabcyl quencher in these cases, although the overall reactivity with SIRT6 was lower than those with SIRT1–3.

18 and **19**, whose quenchers are Dabcyl-BH and Disperse Red, respectively, showed large fluorescence enhancements with SIRT1–3. Because the linker structures of Dabcyl-BH and Disperse Red are longer by one carbon atom than that of Dabcyl-PH, the difference of reactivity of **18** and **19** compared

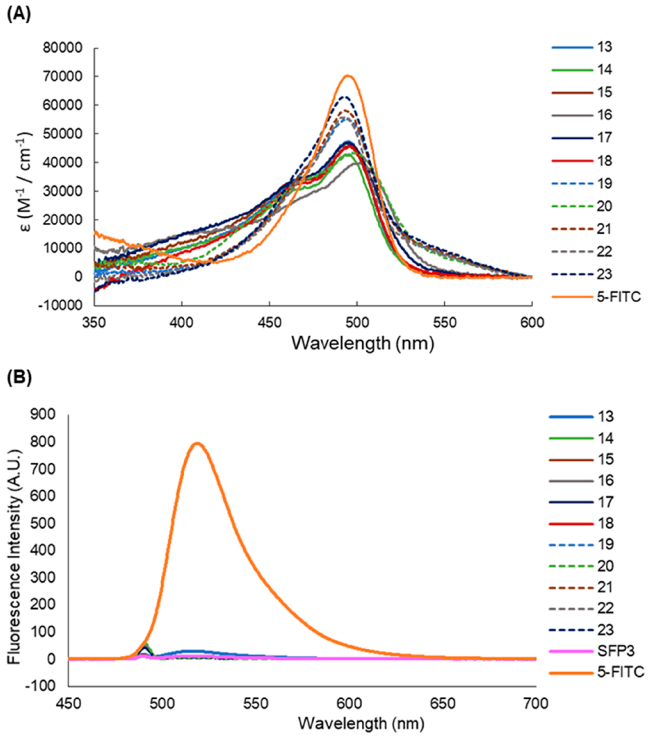

Figure 2. (A) Absorption and (B) fluorescence spectra of 1 μM 5-FITC and **13**–**23**. Data were measured in Tris-buffer (50 mM Tris-HCl (pH 8.0), 150 mM NaCl), containing 0.01% DMSO as a cosolvent.

Table 2. Photophysical Properties of SFP3, 13–23,[a] and 5-FITC

	λ_{max} (nm)	ϵ (10^4 M^{-1} cm^{-1})	λ_{em} (nm)	Φ_{FL}[b]
SFP3	496	8.91	517	0.008
13	496	4.75	516	0.053
14	494	4.26	516	0.014
15	494	5.52	517	0.007
16	499	3.96	516	0.021
17	496	4.69	516	0.018
18	496	4.58	517	0.012
19	496	4.59	517	0.015
20	497	4.34	513	0.005
21	493	5.82	515	0.008
22	493	5.59	515	0.010
23	493	6.31	516	0.006
5-FITC	494	7.04	518	0.696

[a]Data were measured in Tris-buffer (50 mM Tris-HCl (pH 8.0), 150 mM NaCl). [b]For determination of Φ_{FL}, fluorescein in 0.1 N NaOH (Φ_{FL} = 0.85) was used as a fluorescence standard.

with **13** appears to be due to the difference of linker length in the quencher moieties because all three probes have the same peptide chain.

In the case of SIRT1, SFP3 and **13**–**18** showed large fluorescence enhancements regardless of the peptide sequence, suggesting that SIRT1 favors the Dabcyl structure having a dimethylamino group over the Disperse Red structure having a nitro group, except for **16** and **17**, which have peptide sequences optimized for SIRT2. In the case of SIRT2, **18** and **19** showed the greatest fluorescence enhancement, suggesting that SIRT2 precisely recognizes the peptide sequence H4K16. The linker length of the quencher moiety appears to be a key

https://dx.doi.org/10.1021/acsmedchemlett.1c00010
ACS Med. Chem. Lett. 2021, 12, 617–624

Table 3. Fluorescence Enhancement (SIRT(+)/SIRT(−)) of 13−23 and SFP3 with SIRT1−7 after Enzymatic Reaction for 1 h

	SIRT1	SIRT2	SIRT3	SIRT4	SIRT5	SIRT6	SIRT7
SFP3	13.84	5.89	2.20	1.03	1.08	3.60	1.04
13	11.99	5.45	4.00	0.93	1.07	1.33	1.03
14	10.90	4.72	5.45	0.92	1.03	1.05	1.01
15	19.74	6.68	6.55	1.12	1.02	1.04	1.07
16	4.79	1.85	1.92	1.14	1.11	1.07	1.04
17	4.76	1.92	1.96	1.11	1.09	1.05	1.01
18	14.23	12.04	12.48	1.11	1.06	2.21	1.00
19	14.74	10.34	27.23	1.04	1.07	2.55	1.09
20	5.85	6.97	26.71	1.25	1.15	1.19	1.05
21	8.86	5.64	26.18	1.20	1.05	3.36	0.99
22	5.00	3.83	12.31	1.18	0.99	3.51	1.01
23	6.06	4.06	14.07	1.20	1.07	9.38	1.04

factor for high reactivity. As for SIRT3, interestingly, the probes with the Disperse Red quencher (**19**−**23**) showed significantly higher fluorescence enhancement than those with the Dabcyl quencher. Notably, among these probes, **20** and **21** selectively reacted with SIRT3 over SIRT1 and SIRT2.

Overall, these results indicate that our FRET-based fluorescence probes having a quencher dye as a SIRT-hydrolyzable motif are suitable for detecting SIRT1−3 and 6. Moreover, the factors influencing recognition of the fluorescence probes as a substrate by each SIRT subtype are slightly different, suggesting that it is possible to design SIRT-subtype-specific fluorescence probes by precisely optimizing their peptide sequences, quencher structures, and linker lengths.

Determination of the Kinetic Constants of 13−23 with SIRT1−3. To quantitatively evaluate the reactivity of each probe with SIRT1−3, the Michaelis constant (K_m), the catalytic rate constant (k_{cat}), and the specificity constant (k_{cat}/K_m) were determined from Michaelis−Menten plots (Figure 3, Figure S3A−C, Table S1A−C).

For SIRT1, the k_{cat} and K_m values of Dabcyl-type probes (SFP3 and **13**−**18**) are larger than those of Disperse Red-type probes (**19**−**23**), suggesting that Dabcyl-type probes are more efficiently hydrolyzed by SIRT1 than Disperse Red-type probes, though SIRT1 has a higher affinity for the Disperse Red quencher than for the Dabcyl quencher. As a result, the difference of k_{cat}/K_m values for the two quenchers is small.

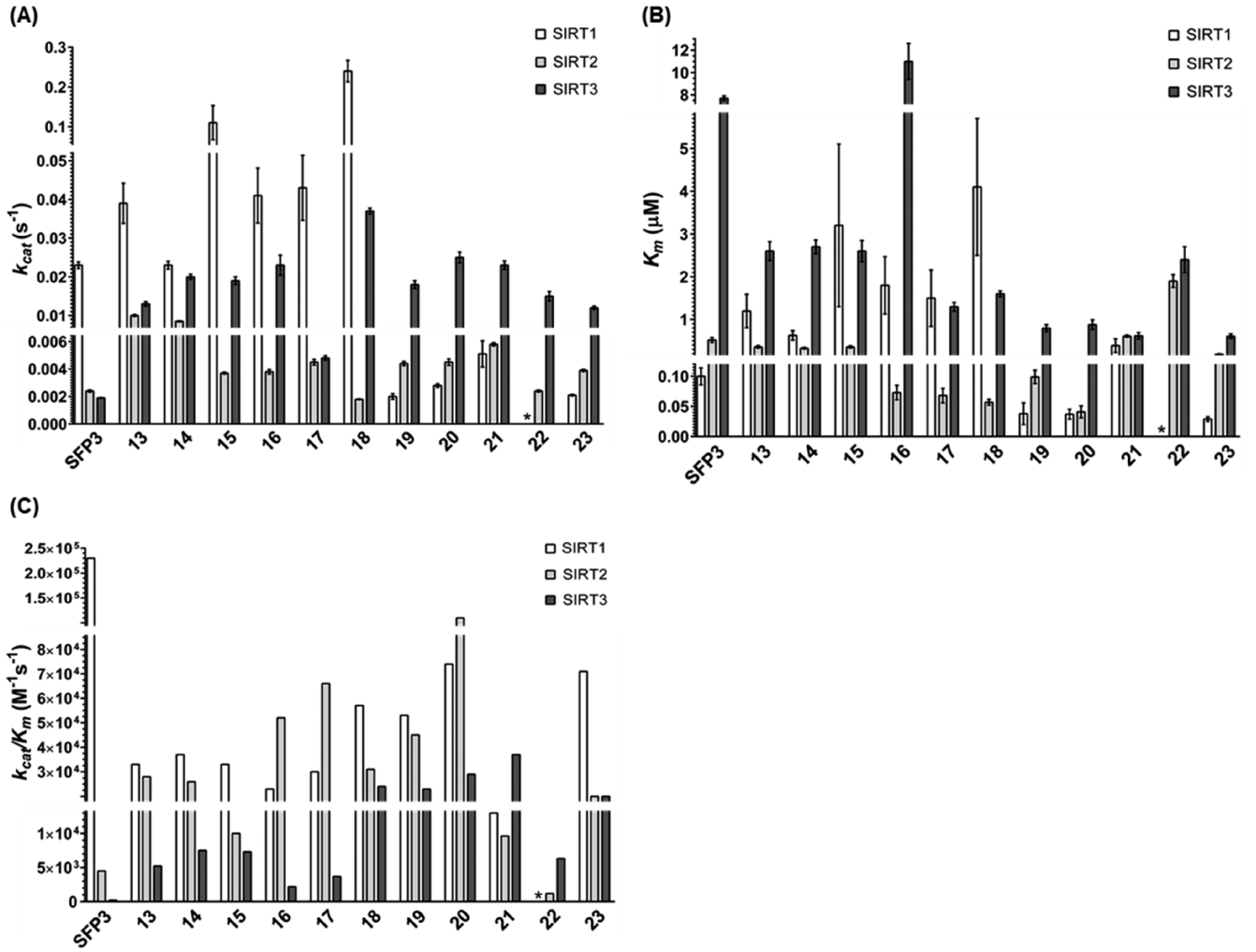

Figure 3. Kinetic parameters of the enzymatic reactions of SIRT1−3 with SFP3 and **13**−**23**. (A) k_{cat} values of each probe. (B) K_m values of each probe. (C) k_{cat}/K_m values of each probe. Asterisks indicate the kinetic parameters of **22** for SIRT1 were not determined. Data for SFP3 were taken from ref 28.

https://dx.doi.org/10.1021/acsmedchemlett.1c00010
ACS Med. Chem. Lett. 2021, 12, 617−624

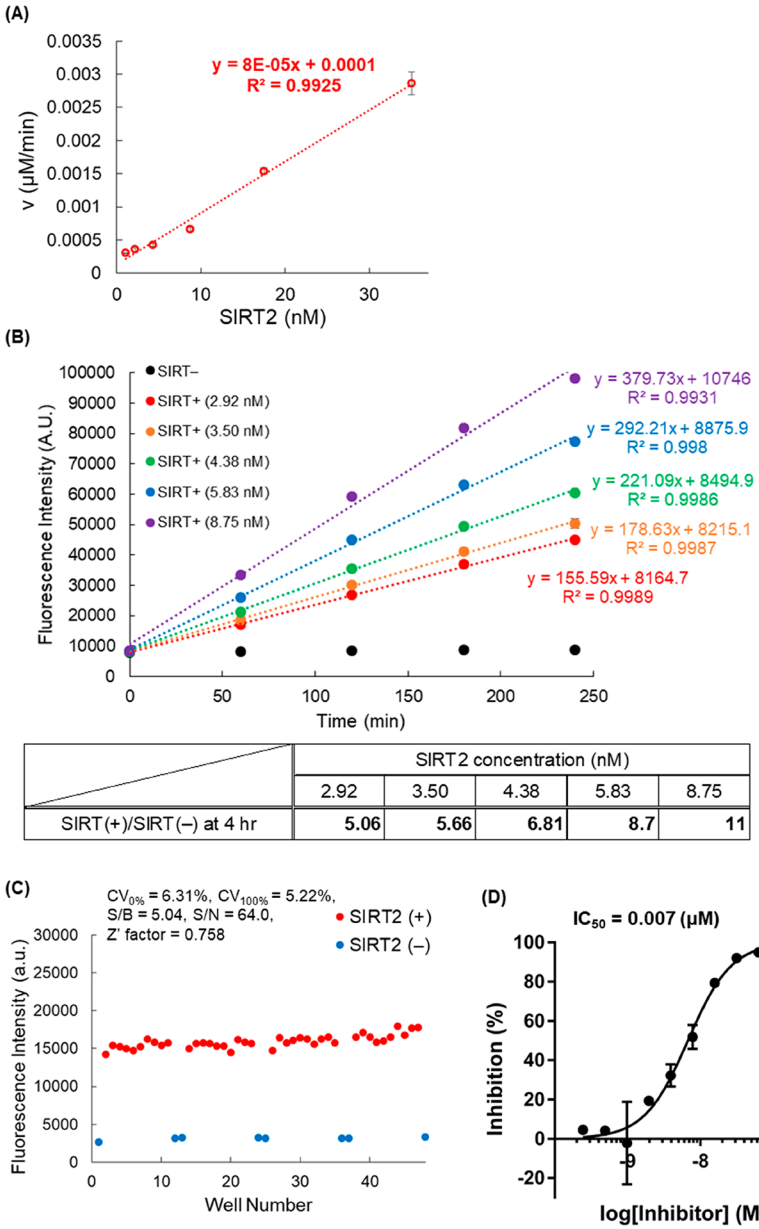

	SIRT2 concentration (nM)				
	2.92	3.50	4.38	5.83	8.75
SIRT(+)/SIRT(–) at 4 hr	**5.06**	**5.66**	**6.81**	**8.7**	**11**

Figure 4. (A) Dependency of the enzymatic reaction rate of **18** on SIRT2 concentration. Results are mean ± SD (n = 3). (B) Time dependence of the enzymatic reaction of **18** with various concentrations of SIRT2 in the range of 2.92−8.75 nM. Results are mean ± SD (n = 3). (C) Reliability of the optimized screening conditions, evaluated in 48 wells of a 96-well half area microplate. CV (coefficient of variation) = SD/Av ≤ 10%; S/B = signal/background ≥3.0; S/N = signal/noise; Z′ factor = $1 - (3 \times SD_{100\%} + 3 \times SD_{0\%})/(Av_{100\%} - Av_{0\%}) \geq 0.5$ for reliable screening. SD = standard deviation, Av = average. (D) Inhibition curve of S2DMi-6 toward SIRT2 obtained with **18**. Results are mean ± SD (n = 3).

Indeed, all the newly developed probes have k_{cat}/K_m values of the order of 10^4.

For SIRT2, the K_m values of **16** and **17**, which contain peptide sequences derived from SIRT2-selective inhibitors, are smaller than those of the other probes with H4K16 sequences. At the same time, the K_m values of **18** and **19** are smaller than that of **13**, suggesting that the longer linker length on the quencher is crucial for higher affinity with SIRT2. **20** showed the highest affinity with SIRT2. However, the k_{cat} values tend to be larger for probes with larger K_m values, and as a result, there is no significant difference in k_{cat}/K_m values among all the probes.

For SIRT3, the k_{cat}/K_m values are of the order of 10^4 for most of the Disperse Red-type probes, i.e., about 10 times larger values than those of the Dabcyl-type probes. This is consistent with the results shown in Table 3, and the higher reactivity of the Disperse Red-type probes with SIRT3 might be attributed to their higher affinity for SIRT3 compared with Dabcyl-type probes. It is noteworthy that the k_{cat}/K_m value of **22** was smaller than those of other Disperse Red-type probes, suggesting that the H2BK12 sequence may not be favorable and that the peptide sequence can influence SIRT3 substrate recognition.

Overall, the effects of quencher structure and peptide sequence on the reaction rate appear to be relatively large, whereas the effect of the peptide length is smaller. Although the newly developed probes have lower reactivity toward SIRT1 than SFP3, they have similar or higher reactivity toward SIRT2 and SIRT3. In particular, **20** and **21** exhibited

https://dx.doi.org/10.1021/acsmedchemlett.1c00010
ACS Med. Chem. Lett. 2021, 12, 617−624

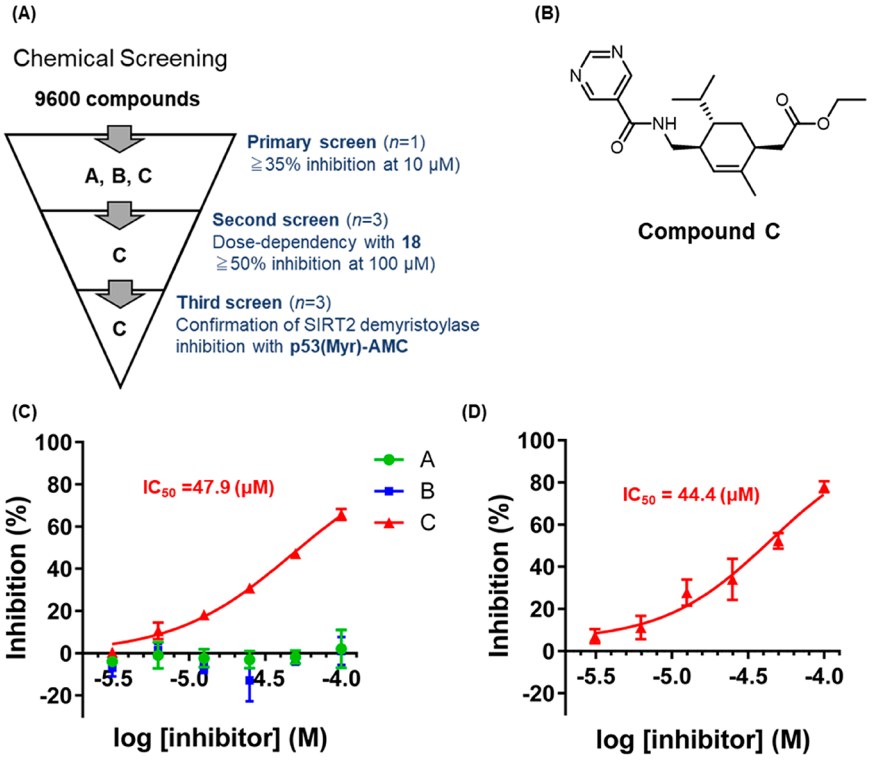

Figure 5. (A) Three-stage screening. (B) Chemical structure of **C**. (C) Inhibition curves of **A**, **B**, and **C** toward SIRT2 obtained with **18**. The results are mean ± SD (n = 3). (D) Inhibition curve of **A** toward SIRT2 obtained with p53(Myr)-AMC. The results are mean ± SD (n = 3).

significantly higher reactivity than SFP3 with SIRT2 (>24-fold) and SIRT3 (>154-fold).

Next, we conducted molecular docking simulations of Dabcyl-PH, Dabcyl-BH, and Disperse Red with the SIRT2 catalytic site (PDB ID: 4X3P) using the CDOCKER algorithm in Discovery Studio Client v17.2.0.16349 (BIOVIA Inc.) (Figure S4). A comparison of the CDOCKER interaction energies of the three quenchers suggests that the binding affinities of Dabcyl-BH and Disperse Red are larger than that of Dabcyl-PH, which is consistent with the K_m values of **13**, **18**, and **19**. Interestingly, all the quenchers share some interactions (e.g., hydrogen bonding with Val233, and $\pi-\pi$ stacking interaction with Phe190), but only Disperse Red can also form a π-cation interaction between its nitro group and Tyr139 (Figure S5A-C).

Validation of an HTS System for SIRT2 Inhibitors Using 18. To illustrate the utility of our newly synthesized probes, we conducted a chemical screening assay to find SIRT2 inhibitors because these would be candidate anticancer agents.[20] Based on the results shown in Table 3, we chose **18** as the most suitable probe for SIRT2 defatty-acylase modulator screening. Initially, we confirmed that the reaction rate of **18** increased linearly with increasing concentration of SIRT (Figure 4A). We next evaluated the time dependence of the enzymatic reaction of **18** with various concentrations of SIRT2 (Figure 4B) and found that the fluorescence increase was linear for at least 4 h. A low concentration of SIRT2 (2.92 nM) was sufficient for SIRT2 activity detection, reflecting the high reactivity of **18**. We further validated the reliability of our screening system with **18** (Figure 4C) by using 48 wells of a 96-well half area plate (SIRT2 (+) in 40 wells and SIRT2 (−) in 8 wells). The $CV_{100\%}$ value was less than 10%, the S/B ratio was more than 3, and the Z' factor was more than 0.5, confirming the reliability of our screening system even with as low a concentration of SIRT2 as 2.92 nM.

We used the established conditions to examine whether **18** can be applied to determine the half-inhibitory activity (IC_{50}) of the reported SIRT defatty-acylase inhibitor S2DMi-6 (Figure 4D, Figure S6A).[29] The measured IC_{50} value was 0.007 μM, which is close to the value given in our previous report (IC_{50} = 0.019 μM, determined by SFP3).[29] In addition, we determined the IC_{50} value of S2DMi-9 toward SIRT6 by using **23** (Figure S6). The measured IC_{50} value was 0.10 μM, which is close to the value given in our previous report (IC_{50} = 0.25 μM, determined with SFP3).[29]

Chemical Screening of SIRT2 Defatty-Acylase Inhibitors Using 18. Following the HTS validation of **18**, we applied it to screen 9600 compounds from a large chemical library for nonpeptide novel SIRT2 defatty-acylase inhibitors (Figure 5A).

Primary screening was performed in 384-well plates, and all compounds were tested at 10 μM in the presence of 0.5% DMSO. This screen yielded three candidate compounds, **A**, **B**, and **C**, which showed more than 35% inhibition at 10 μM (Figure 5B, Figure S7A). We next conducted a second screening with **18** to confirm dose-dependency and to eliminate false-positive compounds (Figure 5C) and found that compound **C** reproducibly inhibited SIRT2 with an IC_{50} value of 47.9 μM. We then conducted a third screening to confirm the SIRT2 defatty-acylase inhibitory activity of the three hit compounds by using our previously developed two-step defatty-acylase probe, p53(Myr)-AMC (Figure S8).[29] Among the three candidates, compound **C** dose-dependently inhibited SIRT2 demyristoylase activity determined with p53(Myr)-AMC, and its IC_{50} value was calculated to be 44.4 μM, in good accordance with the value obtained using **18** (Figure 5D, Figure S7B).

https://dx.doi.org/10.1021/acsmedchemlett.1c00010
ACS Med. Chem. Lett. 2021, 12, 617−624

Further evaluations of compound **C** were conducted to confirm its selectivity for SIRT2 defatty-acylase activity. We found that compound **C** selectively inhibits defatty-acylase activity of SIRT2 over SIRT1, 3, and 6 (Figure S9A). However, compound **C** also inhibited SIRT2 deacetylase activity with an IC_{50} value of 5.09 μM, indicating that it is a dual inhibitor of SIRT2 deacetylase and defatty-acylase activities (Figure S9B).

In addition, we determined the IC_{50} values of known SIRT2 inhibitors, nicotinamide,[31] AGK2,[32] SirReal2,[33] and TM,[34] by using **18** and compared them with those of compound **C** (Figure S10). SirReal2 and TM are much more SIRT2 deacetylase-selective than the classical inhibitors nicotinamide and AGK2. It was found that compound **C** inhibits both SIRT2 deacetylase and defatty-acylase activities, indicating that its defatty-acylase selectivity is similar to those of nicotinamide and AGK2.

Thus, the screening assay with our newly developed, highly sensitive fluorescence probe, **18**, enabled us to identify compound **C** as a nonpeptide, small-molecular SIRT2 defatty-acylase inhibitor.

CONCLUSION

In this research, we designed and synthesized a set of 11 new one-step fluorescence probes with various peptide sequences and quenchers using an improved synthetic scheme that does not involve liquid-phase steps. Evaluation of these probes with SIRT isozymes indicated first that the length of the quencher structure and the peptide sequence are more important factors than peptide sequence length for determining the reaction rate with SIRT1−3, and second, that the Disperse Red quencher is selectively recognized by SIRT3.

Probe-scanning with SIRT isozymes revealed that different combinations of probes and isozymes showed different responses. To illustrate the value of our probe design strategy, we selected compound **18** for HTS application to discover SIRT2 defatty-acylase modulators in a one-step manner. Even with a low concentration of SIRT2, we identified compound **C** as a new, small molecule SIRT2 defatty-acylase inhibitor. Our one-step detection method has the following advantages: (i) low background fluorescence due to the probe's stability, (ii) longer wavelength fluorescence, minimizing possible overlap, (iii) simple manipulation for chemical screening, and (iv) biocompatibility for cellular SIRT activity imaging. A possible drawback is that the substrate recognition sites are different from those of the natural substrates (quenchers vs long-chain fatty acids). However, in our previous paper, we established that IC_{50} values evaluated with our one-step probe are well-correlated with those obtained using a two-step probe, p53(Myr)-AMC, which has a myristoyl group as a substrate recognition site.[29] Therefore, we believe our probe set will be useful to screen chemical libraries for modulators of not only SIRT2 but also other SIRTs, including SIRT1, 3, and 6. Such modulators would be useful tools to decipher the physiological and pathological roles of the defatty-acylase activities of SIRTs as well as to discover new SIRT inhibitors as candidate anticancer therapeutic agents.

ASSOCIATED CONTENT

Supporting Information

The Supporting Information is available free of charge at https://pubs.acs.org/doi/10.1021/acsmedchemlett.1c00010.

Structure of SFP3, reactivity of SFP3 and **13**−**23** with SIRT1−7, Michaelis−Menten plots for SFP3 and **13**−**23** with SIRT1−3, structure of hit compounds A and B and their SIRT2 defatty-acylase inhibitory activity determined by p53(Myr)-AMC, docking simulation of quenchers with SIRT2, selectivity of compound **C** over SIRT1, 3, and 6 and deacetylase activity of SIRT2, inhibitory activities of known SIRT2 inhibitors evaluated with **18**, synthesis of **13**−**23** and *in vitro* experimental procedures (PDF)

AUTHOR INFORMATION

Corresponding Authors

Mitsuyasu Kawaguchi − *Graduate School of Pharmaceutical Sciences, Nagoya City University, Nagoya, Aichi 467-8603, Japan*; orcid.org/0000-0002-1919-1391; Phone: +81-52-836-3408; Email: mkawaguchi@phar.nagoya-cu.ac.jp; Fax: +81-52-836-3408

Hidehiko Nakagawa − *Graduate School of Pharmaceutical Sciences, Nagoya City University, Nagoya, Aichi 467-8603, Japan*; orcid.org/0000-0001-8435-4401; Phone: +81-52-836-3407; Email: deco@phar.nagoya-cu.ac.jp; Fax: +81-52-836-3407

Authors

Yuya Nakajima − *Graduate School of Pharmaceutical Sciences, Nagoya City University, Nagoya, Aichi 467-8603, Japan*

Naoya Ieda − *Graduate School of Pharmaceutical Sciences, Nagoya City University, Nagoya, Aichi 467-8603, Japan*

Complete contact information is available at: https://pubs.acs.org/10.1021/acsmedchemlett.1c00010

Notes

The authors declare no competing financial interest.

ACKNOWLEDGMENTS

The authors thank all the members of H.N.'s laboratory for fruitful discussions and also thank Drs. Hirotatsu Kojima, Takayoshi Okabe, and Tetsuo Nagano at the Drug Discovery Initiative, the University of Tokyo for the assistance of chemical screening. This work was supported in part by JSPS KAKENHI Grants 26893223, 15K18899, and 18K14358 (M.K.) and 16H05103, 19H03354, and 19KK0197 (H.N.) as well as by the Hori Sciences and Arts Foundation (M.K.), a Grant-in-Aid for Scientific Research on Innovative Areas from MEXT (26111012, H.N.) and a grant from Daiichi Sankyo Foundation of Life Science (H.N.). This research was partially supported by the Platform Project for Supporting Drug Discovery and Life Science Research from AMED under Grant JP19am0101086.

ABBREVIATIONS

SIRT, sirtuin; FRET, Förster resonance energy transfer; NAD, nicotinamide adenine dinucleotide; ADP, adenine diphosphate; TNF-α, tumor necrosis factor α; Dabcyl, 4-(4-(dimethylamino)phenylazo)benzoic acid; SPS, solid-phase synthesis; HPLC, high performance liquid chromatography; HTS, high-throughput screening

https://dx.doi.org/10.1021/acsmedchemlett.1c00010
ACS Med. Chem. Lett. 2021, 12, 617−624

REFERENCES

(1) Imai, S.; Armstrong, C. M.; Kaeberlein, M.; Guarente, L. Transcriptional silencing and longevity protein Sir2 is an NAD-dependent histone deacetylase. *Nature* **2000**, *403*, 795−800.

(2) Haigis, M. C.; Guarente, L. P. Mammalian sirtuins−emerging roles in physiology, aging, and calorie restriction. *Genes Dev.* **2006**, *20*, 2913−2921.

(3) Longo, V. D.; Kennedy, B. K. Sirtuins in aging and age-related disease. *Cell* **2006**, *126*, 257−268.

(4) Sauve, A. A.; Wolberger, C.; Schramm, V. L.; Boeke, J. D. The biochemistry of sirtuins. *Annu. Rev. Biochem.* **2006**, *75*, 435−465.

(5) Finkel, T.; Deng, C. X.; Mostoslavsky, R. Recent progress in the biology and physiology of sirtuins. *Nature* **2009**, *460*, 587−591.

(6) Kozako, T.; Suzuki, T.; Yoshimitsu, M.; Arima, N.; Honda, S.; Soeda, S. Anticancer agents targeted to sirtuins. *Molecules* **2014**, *19*, 20295−20313.

(7) Lavu, S.; Boss, O.; Elliott, P. J.; Lambert, P. D. Sirtuins−novel therapeutic targets to treat age-associated diseases. *Nat. Rev. Drug Discovery* **2008**, *7*, 841−853.

(8) Milne, J. C.; Lambert, P. D.; Schenk, S.; Carney, D. P.; Smith, J. J.; Gagne, D. J.; Jin, L.; Boss, O.; Perni, R. B.; Vu, C. B.; Bemis, J. E.; Xie, R.; Disch, J. S.; Ng, P. Y.; Nunes, J. J.; Lynch, A. V.; Yang, H.; Galonek, H.; Israelian, K.; Choy, W.; Iffland, A.; Lavu, S.; Medvedik, O.; Sinclair, D. A.; Olefsky, J. M.; Jirousek, M. R.; Elliott, P. J.; Westphal, C. H. Small molecule activators of SIRT1 as therapeutics for the treatment of type 2 diabetes. *Nature* **2007**, *450*, 712−716.

(9) Guarente, L. Franklin H. Epstein Lecture: Sirtuins, aging, and medicine. *N. Engl. J. Med.* **2011**, *364*, 2235−2244.

(10) Hu, J.; Jing, H.; Lin, H. Sirtuin inhibitors as anticancer agents. *Future Med. Chem.* **2014**, *6*, 945−966.

(11) Feldman, J. L.; Baeza, J.; Denu, J. M. Activation of the protein deacetylase SIRT6 by long-chain fatty acids and widespread deacylation by mammalian sirtuins. *J. Biol. Chem.* **2013**, *288*, 31350−31356.

(12) Huang, H.; Zhang, D.; Wang, Y.; Perez-Neut, M.; Han, Z.; Zheng, Y. G.; Hao, Q.; Zhao, Y. Lysine benzoylation is a histone mark regulated by SIRT2. *Nat. Commun.* **2018**, *9*, 3374.

(13) Roth, M.; Chen, W. Y. Sorting out functions of sirtuins in cancer. *Oncogene* **2014**, *33*, 1609−1620.

(14) Inoue, T.; Hiratsuka, M.; Osaki, M.; Oshimura, M. The molecular biology of mammalian SIRT proteins: SIRT2 in cell cycle regulation. *Cell Cycle* **2007**, *6*, 1011−1018.

(15) Lanyon-Hogg, T.; Faronato, M.; Serwa, R. A.; Tate, E. W. Dynamic protein acylation: new substrates, mechanisms, and drug targets. *Trends Biochem. Sci.* **2017**, *42*, 566−581.

(16) Tate, E. W.; Kalesh, K. A.; Lanyon-Hogg, T.; Storck, E. M.; Thinon, E. Global profiling of protein lipidation using chemical proteomic technologies. *Curr. Opin. Chem. Biol.* **2015**, *24*, 48−57.

(17) Jiang, H.; Khan, S.; Wang, Y.; Charron, G.; He, B.; Sebastian, C.; Du, J.; Kim, R.; Ge, E.; Mostoslavsky, R.; Hang, H. C.; Hao, Q.; Lin, H. SIRT6 regulates TNF-α secretion through hydrolysis of long-chain fatty acyl lysine. *Nature* **2013**, *496*, 110−113.

(18) Jiang, H.; Zhang, X.; Lin, H. Lysine fatty acylation promotes lysosomal targeting of TNF-α. *Sci. Rep.* **2016**, *6*, 24371.

(19) Zhang, X.; Khan, S.; Jiang, H.; Antonyak, M. A.; Chen, X.; Spiegelman, N. A.; Shrimp, J. H.; Cerione, R. A.; Lin, H. Identifying the functional contribution of the defatty-acylase activity of SIRT6. *Nat. Chem. Biol.* **2016**, *12*, 614−620.

(20) Jing, H.; Zhang, X.; Wisner, S. A.; Chen, X.; Spiegelman, N. A.; Linder, M. E.; Lin, H. SIRT2 and lysine fatty acylation regulate the transforming activity of K-Ras4a. *eLife* **2017**, *6*, No. e32436.

(21) Spiegelman, N. A.; Zhang, X.; Jing, H.; Cao, J.; Kotliar, I. B.; Aramsangtienchai, P.; Wang, M.; Tong, Z.; Rosch, K. M.; Lin, H. SIRT2 and lysine fatty acylation regulate the activity of RalB and cell migration. *ACS Chem. Biol.* **2019**, *14*, 2014−2023.

(22) Li, Y.; Liu, T.; Liao, S.; Li, Y.; Lan, Y.; Wang, A.; Wang, Y.; He, B. *Biochem. Biophys. Res. Commun.* **2015**, *467*, 459−466.

(23) Yang, L.-L.; Wang, H.-L.; Yan, Y.-H.; Liu, S.; Yu, Z.-J.; Huang, M.-Y.; Luo, Y.; Zheng, X.; Yu, Y.; Li, G.-B. *Eur. J. Med. Chem.* **2020**, *192*, 112201.

(24) Baba, R.; Hori, Y.; Mizukami, S.; Kikuchi, K. Development of a fluorogenic probe with a transesterification switch for detection of histone deacetylase activity. *J. Am. Chem. Soc.* **2012**, *134*, 14310−14313.

(25) Baba, R.; Hori, S.; Kikuchi, K. Intramolecular long-distance nucleophilic reactions as a rapid fluorogenic switch applicable to the detection of enzymatic activity. *Chem. - Eur. J.* **2015**, *21*, 4695−4702.

(26) Xie, Y.; Yang, L.; Chen, Q.; Zhang, J.; Feng, L.; Chen, J. L.; Hao, Q.; Zhang, L.; Sun, H. Single-stepfluorescent probes to detect decrotonylation activity of HDACs through intramolecular reactions. *Eur. J. Med. Chem.* **2021**, *212*, 113120.

(27) Dai, Q.; Zheng, Z.; Xia, F.; Liu, P.; Li, M. A one-step specific assay for continuous detection of sirtuin 2 activity. *Acta Pharm. Sin. B* **2019**, *9*, 1183−1192.

(28) Kawaguchi, M.; Ikegawa, S.; Ieda, N.; Nakagawa, H. A fluorescent probe for imaging sirtuin activity in living cells, based on one-step cleavage of the Dabcyl quencher. *ChemBioChem* **2016**, *17*, 1961−1967.

(29) Kawaguchi, M.; Ieda, N.; Nakagawa, H. Development of peptide-based sirtuin defatty-acylase inhibitors identified by the fluorescence probe, SFP3, that can efficiently measure defatty-acylase activity of sirtuin. *J. Med. Chem.* **2019**, *62*, 5434−5452.

(30) Morimoto, J.; Hayashi, Y.; Suga, H. Discovery of macrocyclic peptides armed with a mechanism-based warhead: isoform-selective inhibition of human deacetylase SIRT2. *Angew. Chem., Int. Ed.* **2012**, *51*, 3423−3427.

(31) Anthony, A.; Schramm, V. L. Sir2 regulation by nicotinamide results from switching between base exchange and deacetylation chemistry. *Bio Chemistry.* **2003**, *42*, 9249−9256.

(32) Outeiro, T. F.; Kontopoulos, E.; Altmann, S. M.; Kufareva, I.; Strathearn, K. E.; Amore, A. M.; Volk, C. B.; Maxwell, M. M.; Rochet, J.-C.; McLean, P. J.; Young, A. B.; Abagyan, R.; Feany, M. B.; Hyman, B. T.; Kazantsev, A. G. Sirtuin 2 inhibitors rescue alpha-synuclein-mediated toxicity in models of Parkinson's disease. *Science* **2007**, *317*, 516−519.

(33) Rumpf, T.; Schiedel, M.; Karaman, B.; Roessler, C.; North, B. J.; Lehotzky, A.; Oláh, J.; Ladwein, K. I.; Schmidtkunz, K.; Gajer, M.; Pannek, M.; Steegborn, C.; Sinclair, D. A.; Gerhardt, S.; Ovádi, J.; Schutkowski, M.; Sippl, W.; Einsle, O.; Jung, M. Selective Sirt2 inhibition by ligand-induced rearrangement of the active site. *Nat. Commun.* **2015**, *6*, 6263.

(34) Jing, H.; Hu, J.; He, B.; Negron Abril, Y. L.; Stupinski, J.; Weiser, K.; Carbonaro, M.; Chiang, Y.-L.; Southard, T.; Giannakakou, P.; Weiss, R. S.; Lin, H. A SIRT2-selective inhibitor promotes c-Myc oncoprotein degradation and exhibits broad anticancer activity. *Cancer Cell* **2016**, *29*, 767−768.

https://dx.doi.org/10.1021/acsmedchemlett.1c00010
ACS Med. Chem. Lett. 2021, 12, 617−624